Available online at www.sciencedirect.com
ScienceDirect
Journal of Catalysis 246 (2007) 100–108
JOURNAL OF CATALYSIS
www.elsevier.com/locate/jcat

Support effects in CoMo hydrodesulfurization catalysts prepared with EDTA as a chelating agent

Mohan S. Rana [a], Jorge Ramírez [a,b,*], Aída Gutiérrez-Alejandre [b], Jorge Ancheyta [a], Luis Cedeño [b], S.K. Maity [a]

[a] *Instituto Mexicano del Petróleo, Eje Central Lázaro Cárdenas 152, México City, 07730, Mexico*
[b] *UNICAT, Departamento de Ingeniería Química, Facultad de Química, UNAM, Cd. Universitaria, México, DF 04510, Mexico*

Received 7 July 2006; revised 21 November 2006; accepted 22 November 2006
Available online 26 December 2006

Abstract

The support effect was analyzed for hydrodesulfurization CoMo catalysts prepared with EDTA as the chelating agent. Supports with different isoelectric points, γ-Al_2O_3, Al_2O_3–MgO, and SiO_2, were used. Different sequences of EDTA, Co, and Mo impregnation were used to analyze whether the sequence of addition affected catalytic activity. Changing the order of addition of Co, Mo, and EDTA produced only a small effect on the catalyst HDS activity. The simultaneous impregnation of Co, Mo, and EDTA led to higher HDS activity than sequential impregnations. In contrast, changing the support nature produced important variations in catalytic activity, following the increasing order: $Al_2O_3 < SiO_2 < Al_2O_3$–MgO. It was found that the changes in HDS activity with the type of support are related to different levels of promotion of Mo by Co, and to changes in the sulfidation patterns induced by different interactions of the active phase precursors with each support.

Keywords: CoMo HDS catalyst; Support effect; Al_2O_3; SiO_2; Al_2O_3–MgO; EDTA; Chelating agent

1. Introduction

In recent years, increasingly strict environmental legislation on transportation fuel quality has been implemented or planned worldwide [1]. In particular, the allowable sulfur content in transportation fuels will evolve to near zero in the near future. Consequently, hydrodesulfurization (HDS) catalysts with improved activity, selectivity, and/or stability are needed. Important improvements in the performance of HDS catalysts have been achieved by changing the nature of the catalyst support [2–9], or modifying the catalyst preparation method. The interactions between metallic phases and support have an important influence on the dispersion, morphology, and performance of the active phase. On the other hand, careful control during catalyst preparation is crucial to optimize the incorporation of the Co and Mo active ingredients into the HDT catalyst to achieve high catalytic activity.

The active phase of HDS catalysts is usually composed of nanocrystallites of MoS_2 or WS_2 promoted by Co, Ni, or both [3]. Formation of an effective active phase is achieved when the promoter is located at the edges and corners of the MoS_2 crystallites. Therefore, the catalyst preparation method is crucial for achieving high activity; if instead of interacting closely with the edges of the MoS_2 crystallite, the Co promoter remained isolated, it could react with the support, forming $CoAl_2O_4$, or, during sulfidation, which occurs at low temperature (∼180 °C) [10], forming inactive Co_9S_8. Recently, several groups have reported important improvements in the performance of HDS catalysts using chelating agents during catalyst preparation [11–30]. Their findings indicate that when a chelating agent is added to the impregnating solutions containing the Ni (or Co) and Mo precursors, the formation of a Co(Ni)-chelating ligand complex retards the sulfidation of the Co or Ni promoter beyond the sulfidation of Mo, leading to efficient promotion of the MoS_2 phase and diminished formation of bulk Co or Ni sulfides.

* Corresponding author. Fax: +52 55 56225366.
E-mail address: jrs@servidor.unam.mx (J. Ramírez).

0021-9517/$ – see front matter
doi:10.1016/j.jcat.2006.11.025

There is a vast literature on catalysts prepared by conventional methods; several authors have reviewed the most important findings on the support effects [2,4–7,31,32]. However, support effects when using chelating agents in catalyst preparation have been reported in few cases and are not yet clearly understood [11,15]. Rycskowski [33] has investigated some features of the interactions between chelate molecules and supports in a study of the interaction of EDTA alkaline salts with the surface of inorganic solids. It was found that the type of hydroxyl groups and the isoelectric point of the inorganic oxide supports have a noticeable affect on the nature of the EDTA complex–support oxide interactions. The chemical state of the resulting Mo species is also strongly influenced by the nature of the support [34]. Therefore, it is highly likely that the nature of the support oxide can change the sulfidation pattern of the Co–EDTA complex and the Mo precursor (AHM), thereby affecting catalyst HDS activity.

To investigate further the support effect when EDTA is used as a chelating agent in catalyst preparation, in the present work we synthesized CoMo–EDTA catalysts supported on oxides with different isoelectric points (Al_2O_3, Al_2O_3–MgO, SiO_2) and tested them in the HDS of thiophene. Nitrogen physisorption, high-resolution transmission electron microscopy (HRTEM), temperature-programmed sulfidation (TPS), and NO and CO chemisorption analyzed by infrared were used to characterize the textural properties of the catalysts; dispersion of the MoS_2 phase, patterns of sulfidation, and the relative number and type of coordinatively unsaturated sites (CUS) present in the sulfided catalysts.

2. Experimental

Al_2O_3–MgO (10 wt% of MgO) was prepared by homogeneous precipitation using aqueous aluminum nitrate (2 M) and magnesium nitrate (2 M) as precursors, and 10 wt% solution of NH_4OH as a precipitating agent [35]. Pure alumina was prepared by the urea hydrolysis method using $Al(NO_3)_3$ as precursor salt [36]. Extrudates of the precipitates were dried at room temperature for 12 h, then at 120 °C for 12 h, and were finally calcined at 550 °C for 4 h.

Mesoporous silica was synthesized from a gel with composition 4.0 SiO_2:1.0 cetyltrimethylammonium bromide (CTABr): 1.5 Na_2O:0.15 $(NH_4)_2O$:200 H_2O at pH 10. The mixture of the above compounds was digested in a Teflon-coated autoclave at 97 °C for 24 h. The resulting solid was separated by filtration, washed with 1 L of deionized water on the filter, and dried at room temperature overnight. The solid was further dried at 120 °C for 12 h and calcined at 500 °C for 5 h.

CoMo and CoMo–EDTA catalysts were prepared by the incipient wetness impregnation of solutions containing the Co, Mo, and EDTA salts. Three different sequences of impregnation were used for the preparation of CoMo–EDTA-supported catalysts. In the first (co-impregnation of Co, Mo, and EDTA), the latter was first dissolved in a concentrated NH_4OH solution, to which aqueous cobalt nitrate was added; after the color of the solution changed from reddish to dark reddish, a required amount of a basic solution of AHM was added. The resulting solution was used to impregnate the support. In the second preparation (Mo first and Co + EDTA after), an aqueous solution containing the Mo precursor, AHM, was impregnated first, followed after drying by impregnation with $Co(NO_3)_2$ and EDTA dissolved in a concentrated NH_4OH solution. In the third preparation (Co first and Mo + EDTA after), an aqueous solution of $Co(NO_3)_2$ was impregnated first, followed after drying by impregnation of AHM and EDTA dissolved in concentrated NH_4OH solution. In all of these preparations, a molar ratio of EDTA/Co = 1.2 was used and a pH of 9 was maintained during the incorporation of EDTA, because EDTA–Co forms a stable complex at pH > 8 [37]. The solids obtained from these preparations were dried under air at room temperature (12 h), and then at 120 °C for 12 h. A low Mo content (8 wt% Mo) was used to obtain coverages below the monolayer capacity for all supports. The Co content was adjusted to maintain an atomic ratio Co/(Co + Mo) = 0.33. Hereinafter, the simultaneously prepared catalysts are designated CoMoE, those with Co first and Mo + EDTA after are designated Co(Mo + E), and those with Mo first and Co + EDTA after are designated Mo(Co+E).

Measurement of BET specific surface area, pore volume, and pore size distribution was carried out by nitrogen physisorption at −196 °C using Quantachrome Nova 2000 equipment. Before nitrogen adsorption, the samples were outgassed 3 h at 300 °C.

Analysis of the chemisorption of NO and CO over the sulfided catalysts was performed with a Nicolet 760 model FTIR spectrometer with a resolution of 2 cm^{-1} and 200 scans per spectrum. For the analysis, the powdered catalyst samples were pressed into self-supporting wafers (10–14 mg/cm^2) and then sulfided in a high-vacuum glass cell connected to a gas manipulation manifold using a flow of 20 mL/min of H_2S/H_2 (15% v/v) mixture for 4 h at 400 °C. The sulfided sample was pretreated by outgassing for 2 h at 400 °C. For NO adsorption, a pulse of NO was introduced (50 Torr) at room temperature to the IR cell, and the spectra were collected. For the adsorption of CO at low temperature (−173 °C), small doses of CO were introduced into the cell until an equilibrium pressure of 1 Torr was reached. After each pulse, the corresponding spectrum was obtained.

HRTEM observations of sulfided catalysts were performed with a JEOL JEM-2010 microscope operated at 200 kV. Samples were milled in an agate mortar and ultrasonically suspended in *n*-heptane. A drop of the supernatant liquid was placed on a copper grid coated with a sputtered carbon polymer. For the estimation of average length and stacking of MoS_2 more than 200 crystallites were measured.

Raman experiments were performed on the unsulfided samples using a NICOLET Almega XR Dispersive Raman Spectrometer with 50 s of scanning time and resolution of 4 cm^{-1}.

TPS experiments were performed using a sulfiding mixture containing 5% H_2S and 95% H_2 (flow rate, 10 mL/min). H_2S was detected in the effluent gas with a UV spectrophotometer set at 200 nm and equipped with a flow cell. During TPS, the temperature was increased at a rate of 10 °C/min up to a final temperature of 400 °C, where it was maintained for 30 min.

The catalyst activity was evaluated in the HDS of thiophene at 400 °C and atmospheric pressure. In a typical experiment,

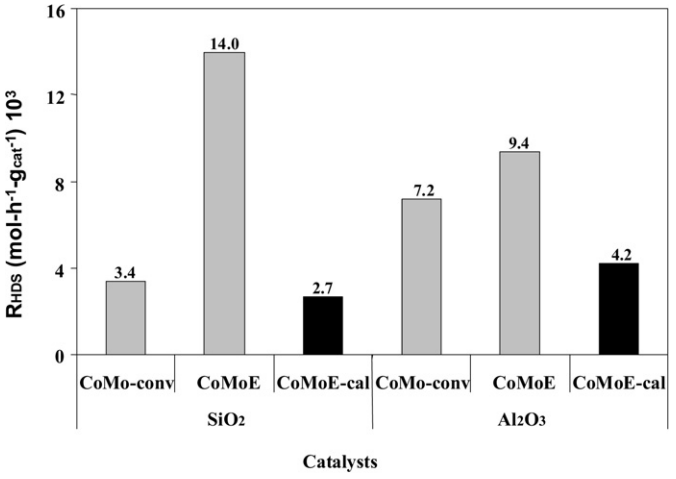

Fig. 1. Thiophene HDS activity for SiO_2- and Al_2O_3-supported CoMo catalysts prepared with and without chelating agent (EDTA). CoMoE-calc was calcined (400 °C, 4 h) prior to sulfidation. CoMo-conv was prepared without EDTA following a conventional preparation method (impregnation–drying–calcination).

100 mg of catalyst (0.4–0.8 mm) was loaded into the glass fixed-bed reactor (0.8 cm i.d.). Before the activity test, the catalyst was sulfided with a mixture of H_2S/H_2 (8–10 vol% of H_2S), at a heating rate of 1 °C/min from room temperature to 400 °C, and the catalyst was maintained at this temperature for 4 h. The purpose of the low heating rate was to avoid rapid thermal decomposition of the Co–EDTA complexes. For the thiophene HDS experiments, a flow of H_2 (100 mL/min) containing 4.7 mol% thiophene was used as feed to the reactor. The conversion of thiophene was kept below 15% to operate in differential regime. Reaction rates were calculated according to the equation $r = x(F/W)$, where r is the reaction rate of thiophene (in mol/(h g)), x is thiophene conversion, W is the weight of the catalyst (in g), and F is the flow rate of reactant (in mol/h) [38].

3. Results and discussion

3.1. Catalytic activity

3.1.1. Effect of the chelating agent (EDTA)

The role of the chelating agent during catalyst preparation is to form a stable complex with the Co promoter to delay its sulfidation beyond that of the Mo phase to achieve a good level of interaction between Co and the MoS_2 crystallites and avoid the formation of excessive bulk Co sulfide. The importance of maintaining the Co-chelating agent interaction is clearly shown when calcination is performed before sulfidation. In this case, the chelating agent in the Co–EDTA complex is destroyed during calcination, causing an earlier transformation of the Co phase, which sulfides before the formation of the MoS_2 phase; this results in lower promotion of MoS_2 by Co and poor HDS activity, as shown in Fig. 1 for $CoMoE/SiO_2$ and $CoMoE/Al_2O_3$ prepared with and without calcination. For comparison, Fig. 1 also shows the activity of similar catalysts prepared with calcination and without the use of chelating agent. For SiO_2-supported catalysts, the HDS activity of the catalyst prepared without EDTA and that of the calcined catalyst are similar, indicating that when the Co–EDTA complex is destroyed before sulfidation, no benefit is achieved by the use of the EDTA ligand. In contrast, the activity of the uncalcined CoMoE catalyst is five times higher than that of the calcined one. However, for this catalyst, the interaction between the silica support and the Mo precursor is low; thus, it is possible that calcination leads to much lower Mo dispersion and that the observed differences in catalytic activity do not strictly reflects the sole influence of EDTA. It is then possible that the drop in HDS activity due to calcination becomes lower when a more interactive support, like alumina, is used.

Fig. 1 shows a drop in HDS activity of 56% when $CoMoE/Al_2O_3$ is calcined before sulfidation, compared with 81% when $CoMoE/SiO_2$ is calcined. Nevertheless, the activity trends displayed by the alumina-supported catalysts prepared with and without calcination are similar to those observed for the SiO_2-supported catalysts, although the levels of activity are different. The differences in activity between these two types of catalysts can be ascribed to several effects. The higher activity of conventional and CoMoE-calcined catalysts supported on alumina compared to the corresponding SiO_2-supported ones is most probably due to the better dispersion obtained on the alumina-supported catalysts due to the stronger interaction of the Mo oxide phases with the alumina support. It recently has been shown that because of the interactions of EDTA with the alumina support, better Ni and Mo dispersion is obtained during the impregnation step [39].

The lower activity observed for the $CoMoE/Al_2O_3$ catalyst with respect to its SiO_2-supported counterpart could be due to the partial formation of Anderson-type $AlMo_6$ entities, evidenced in the Al_2O_3-supported catalyst, before sulfidation, by the presence of Raman peaks at 352 and 381 cm^{-1} (results not shown), assigned to the bending modes of terminal M=O bonds in $AlMo_6$ heteropolyanions. Formation of Anderson-type compounds has been reported on alumina-supported catalysts when chelating agents are used in the catalyst preparation [40]. They also have been detected when ammonium heptamolybdate is deposited on γ-alumina by the equilibrium adsorption method [41]. The greater interaction of the Mo species with the alumina support could be the cause of the observed smaller positive effect on the HDS activity caused by use of the chelating agent in the preparation of alumina-supported catalysts compared with those supported on SiO_2. A modest effect of the chelating agent on HDS (13% increase) for alumina supported CoMo catalysts was also recently reported for the hydrodesulfurization of heavy gas oil [42].

3.1.2. Effect of the order of Co, Mo, and EDTA addition

To investigate the effect of the order of addition of Co, Mo, and EDTA (E), three different sequences of catalyst preparations—CoMoE, Co(Mo + E), and Mo(Co + E), all supported on alumina—were tested in the thiophene HDS reaction. The results, presented in Table 1, indicate that the order of addition of Co, Mo, and EDTA caused only small differences in the HDS activity of the catalysts, which follow the order (CoMoE) > Mo(Co + E) > Co(Mo + E). The lowest activity of

Table 1
Effect of Co, Mo, and EDTA order of impregnation and support composition (Al_2O_3–MgO, SiO_2, and Al_2O_3) on thiophene HDS activity

Catalysts	Rate (mol/(h g_{cat})), 10^3
Impregnation method	
$CoMoE/Al_2O_3$	9.3
$Mo(Co + E)/Al_2O_3$	8.4
$Co(Mo + E)/Al_2O_3$	7.7
Support effect	
$CoMoE/Al_2O_3$	9.4
$CoMoE/SiO_2$	14.0
$CoMoE/Al_2O_3$–MgO	20.1

Co(Mo + E) can be explained by the difficulty of formation of the Co–EDTA complex because in this preparation method the Mo–EDTA complex, added in the second step of the impregnation, will have some diffusional limitations in reaching all of the sites where Co was initially deposited, especially in the case of small pores. Once the Co^{2+} ion is close to the Mo–EDTA complex, replacement of Mo by Co is fast, due to the large difference in stability constants between Co–EDTA and Mo–EDTA. Nevertheless, although the solubility of $Co(NO_3)_2$ is high, with this sequence of impregnation, there will be some diffusional limitations to achieving homogeneous concentration of the Co–EDTA complex along the length of the support pores. It is highly probable then that in this catalyst, the radial concentration profile of Co will be uniform, but that of Mo and EDTA will not be, thus leading to different Co/Mo ratios along the length of the pore. In this case, the fraction of Co not complexed by EDTA will sulfide at low temperature, before MoS_2 formation occurs, and will have a greater probability of forming the inactive phase Co_8S_9.

For Mo(Co + E), the Co–EDTA complex is formed in the impregnating solution before the Mo-containing support is impregnated. In this case, the intimacy of contact between Mo and Co–EDTA will depend on the effectiveness of the diffusion of the Co–EDTA complex inside the small pores where Mo is already impregnated and on the level of pore blocking caused during Mo impregnation. Because Mo is impregnated first followed by drying, it is also possible that the interactions of the Mo precursor salt, AHM, with the alumina support will affect the sulfidation of Mo.

For the CoMoE preparation, intimate contact of Mo and Co–EDTA is achieved in solution before the support is impregnated; thus, although some difference in the diffusion coefficients of the Mo and Co precursors is expected, differences in the Co/Mo concentration ratios along the pores will be minimized when both precursors are introduced simultaneously into the support. Moreover, the capillarity forces during the impregnation process also will help minimize the possible variations in radial concentration caused by differences in the diffusion coefficients of the two precursors. Accordingly, the catalyst prepared by this method would be expected to exhibit the most effective promotion of Mo by Co.

Complete complexation of Co by EDTA will effectively delay its sulfidation beyond that of Mo and allow effective promotion of the MoS_2 phase. The delay in the sulfidation of the active phase precursors from the use of chelating agents during catalyst preparation has been reported for NiMo and NiW catalysts [14,16,43]. A greater delay in the sulfidation of Co with respect to that of Mo allows more efficient decoration of the MoS_2 crystallite edges and thereby better Co promotion. As a result, the likelihood of formation of bulk cobalt sulfide, Co_9S_8, is lower during sulfidation in the simultaneously impregnated catalyst than in the sequential preparations. Other possible explanation of the higher activity of the co-impregnated (CoMoE) catalysts could be that this preparation method favors formation of CoMoS-II type structures.

3.1.3. Effect of support

The effect of the support on the activity of CoMoE catalysts was studied using three supports with different isoelectric points: γ-Al_2O_3 (IEP = 8.5), mesoporous SiO_2 (IEP = 2.0), and Al_2O_3–MgO (IEP = 9.0). The activity of CoMoE catalysts over the three supports was evaluated in the thiophene HDS reaction; the results are reported in Table 1. $CoMoE/Al_2O_3$ was the least active catalyst, followed by $CoMoE/SiO_2$ and $CoMoE/Al_2O_3$–MgO in increasing order. The latter catalyst is twice as active as $CoMoE/Al_2O_3$, indicating an important effect of the nature of the support on the activity of the catalyst. To analyze whether the observed differences in activity were due to differences in the dispersion of the MoS_2 phase or in the level of promotion of the MoS_2 crystallites by Co, the sulfided catalysts were characterized by several techniques. HRTEM analysis was used to estimate the relative dispersion of the MoS_2 phase, while the level of promotion was assessed from the NO and CO chemisorption results. The sulfidation behavior of the Co and Mo surface species was followed by TPS experiments.

4. Catalyst characterization

4.1. Textural properties

Specific BET surface areas (SSAs) and pore volumes (PVs) of supports (γ-Al_2O_3, Al_2O_3–MgO, and SiO_2) and catalysts (dried and after reaction) are given in Table 2. The dried catalysts show about 80% decrease in SSA and PV compared with the support. This could be explained by substantial pore blocking caused by the Co–EDTA complex. However, Co–EDTA decomposed during sulfidation, leaving a Co sulfide phase on the surface. Accordingly, after sulfidation and reaction, the SSA and PV of catalysts were similar to the corresponding supports

Table 2
Textural properties of supports and catalysts, dried and after reaction

Support	Support		CoMoE dried		CoMoE after reaction	
	SSA[a]	PV[b]	SSA	PV	SSA	PV
Al_2O_3	141	0.42	29	0.12	118	0.31
Al_2O_3–MgO	197	0.41	53	0.08	162	0.35
SiO_2	489	0.54	95	0.09	382	0.45

[a] SSA: specific surface area (m^2/g).
[b] PV: pore volume (mL/g).

Table 3
Average length (L_{av}) and stacking (N_{av}) of MoS_2 crystallites

Catalyst	L_{av} (Å)	N_{av}
$CoMoE/Al_2O_3$	46	1.4
$CoMoE/Al_2O_3$–MgO	39	1.3
$CoMoE/SiO_2$	56	2.6

(see Table 2), indicating good dispersion of the active sulfided phases.

4.2. High resolution transmission electron microscopy (HRTEM)

The dispersion and morphology of MoS_2 crystallites in HDS sulfided catalysts can be analyzed by HRTEM. With this technique it is possible to visualize the typical lattice fringes representing the basal plane of MoS_2 structures with ∼6.2 Å interplanar distances. Average length (L_{av}) and number of layers (N_{av}) for the MoS_2 crystallites on each support were estimated after measuring several hundred particles on enlarged micrographs (see Table 3). Fig. 2 shows the micrographs of the MoS_2 crystallites present in each catalyst. On alumina, the average length (L_{av}) of MoS_2 crystallites, 46 Å, is in agreement with the typical length observed in MoS_2/Al_2O_3 catalysts [44]. For Al_2O_3–MgO, shorter MoS_2 crystallites with average length 39 Å are observed. For these two supports, the average stacking (N_{av}) of MoS_2 crystallites is slightly above one layer. In contrast, on SiO_2, longer ($L_{av} = 56$ Å) and more stacked ($N_{av} = 2.6$) MoS_2 crystallites are observed.

The dispersion of Mo and Co (Ni) on different supports will depend on, among several other factors, the strength of the interaction between the precursors of the active phase and the support. When chelating agents are used, the interaction of the ligand with the support also may be important. The differences in interaction strength between the EDTA carboxyl groups and the hydroxyl groups for various supports (SiO_2, TiO_2, MgO, Al_2O_3, ZrO_2, and others) were revealed in a recent study by Rycskowski [33]. That study also reported that the isoelectric point (IEP) of the inorganic oxide support has an important influence on the chelate–support interaction. Because SiO_2 has an IEP of ∼2.0, Al_2O_3 of ∼8.5, and MgO of ∼12, significant differences in the chelate–support interaction are envisaged. In accordance with that previous study [33], the ability of EDTA to interact with the inorganic oxide supports used here is $SiO_2 < MgO < Al_2O_3$.

HRTEM (Fig. 2 and Table 3) shows that smaller MoS_2 crystallites are formed on $CoMoE/Al_2O_3$–MgO. The average length of MoS_2 crystallites is 39 Å on this support, compared with 46 Å on alumina and 56 Å on silica. The level of stacking of MoS_2 crystallites also varies with the support. The average number of layers is 1.3 for $CoMoE/Al_2O_3$–MgO, 1.4 for $CoMoE/Al_2O_3$, and 2.6 for $CoMoE/SiO_2$. According to these results, MoS_2 dispersion follows the trend: $CoMoE/Al_2O_3$–MgO > Al_2O_3 > SiO_2, which does not coincide fully with the catalytic activity ranking, indicating that for the catalysts used here, dispersion of the MoS_2 phase is not the key parameter controlling the catalyst HDS activity.

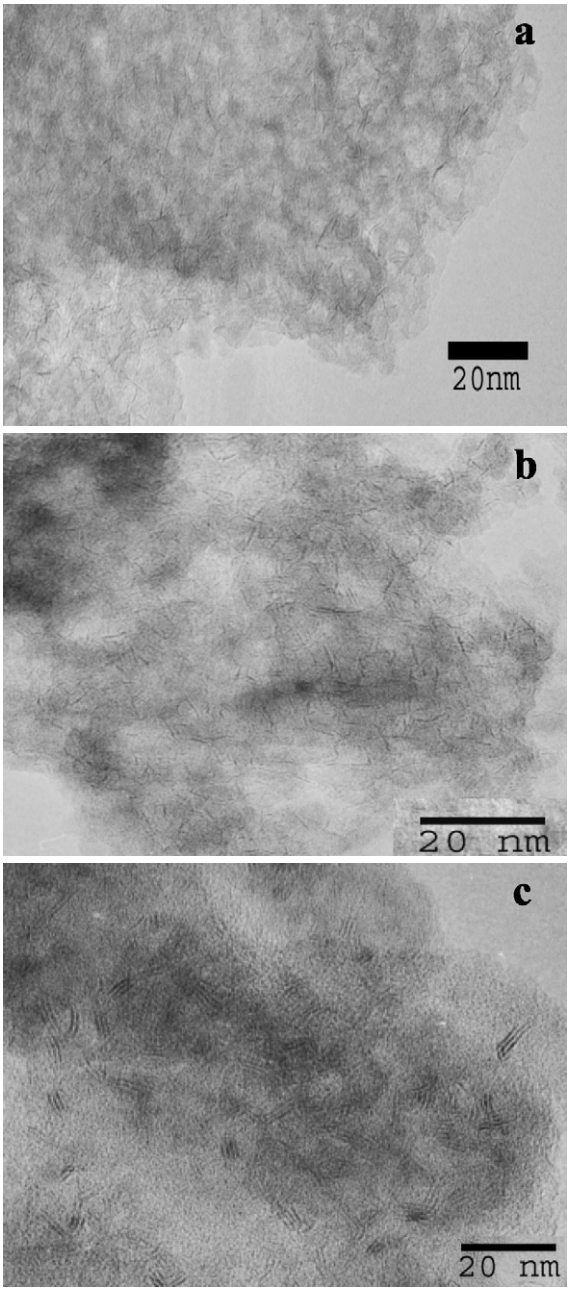

Fig. 2. HRTEM micrographs of MoS_2 crystallites present in (a) $CoMoE/Al_2O_3$, (b) $CoMoE/Al_2O_3$–MgO, and (c) $CoMoE/SiO_2$.

4.3. FTIR characterization

4.3.1. NO adsorption

Chemisorption of NO over CoMo sulfided catalysts provides useful information about the Mo and Co exposed sites because these molecules selectively adsorb on the coordinative unsaturated cobalt (CUS–Co) and molybdenum (CUS–Mo) sites [45,46]. Because the materials under study present widely different transmittance levels to the IR laser beam, quantitative comparison of the absolute numbers of Co and Mo sites is difficult and not completely reliable. To partially overcome this problem, it was decided to evaluate the level of promotion for each catalyst. Toward this end, the ratio CUS–Co/CUS–Mo (for NO

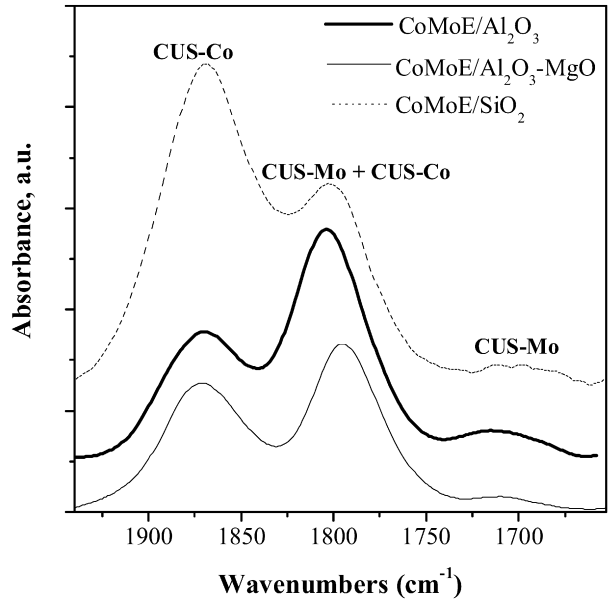

Fig. 3. FTIR spectra of NO adsorbed in the N–O stretching region for CoMoE sulfided catalysts on different supports.

adsorption) or CUS–CoMoS/CUS–Mo (for CO adsorption, see below), which give a measure of the availability of sulfur vacancies associated to Co sites (total or promoted, respectively), divided by those associated to unpromoted Mo sites, was evaluated in each spectrum. One drawback of this approach is that at close to 100% promotion, the ratio of promoted sites to unpromoted sites increases drastically. In the particular case of NO adsorption, analysis of the CUS–Co/CUS–Mo ratio must be exercised with caution, because NO adsorption does not distinguish between Co promoted from other Co sites present in such phases as Co_9S_8.

Fig. 3 shows the IR spectra of NO adsorption in the N–O stretching region for the sulfided catalysts supported on Al_2O_3, Al_2O_3–MgO, and SiO_2. All of the IR spectra show the presence of three bands at about 1705, 1800, and 1870 cm^{-1}. According to literature reports [45], the bands at ∼1705 and ∼1800 cm^{-1} are assigned to ν_{as} and ν_s stretching vibration modes of NO adsorbed on CUS–Mo sites, whereas those at ∼1800 and ∼1870 cm^{-1} are assigned to ν_{as} and ν_s stretching vibration modes of NO adsorbed on CUS–Co. In view of the overlapping of the ν_{as} and ν_s modes of NO adsorbed on Co and Mo respectively, only the higher-frequency (∼1870 cm^{-1}) and lower-frequency (∼1705 cm^{-1}) bands are considered for Co and Mo analysis. Shimizu et al. [47] reported similar band frequencies for Mo and slightly lower ones for Co (1840 cm^{-1}) for HDS catalysts prepared with EDTA.

In our case, the spectra of NO adsorbed on the different sulfided catalysts (Fig. 3) indicate that the amount of NO adsorbed on CUS–Mo increases in the order $CoMoE/SiO_2$ ∼ $CoMoE/Al_2O_3$ > $CoMoE/Al_2O_3$–MgO. Because NO adsorption on the Mo sites and catalytic activity trends differ, it appears that dispersion of the MoS_2 phase does not determine catalyst activity. However, we observed changes in the CUS–Co/CUS–Mo bands intensity ratio. For our catalysts, the higher intensity of the CUS–Co band (∼1870 cm^{-1}) in all samples

Table 4
Level of promotion estimated from NO and CO adsorption experiments on sulfided catalysts

Catalyst	CUS–Co/CUS–Mo (NO adsorption)	CUS–CoMoS/CUS–Mo (CO adsorption)
$CoMoE/Al_2O_3$	4.1	0.6
$CoMoE/Al_2O_3$–MgO	74.3	3.2
$CoMoE/SiO_2$	49.0	1.4

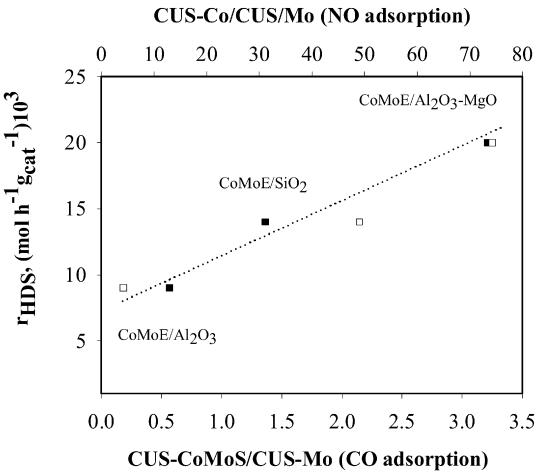

Fig. 4. Thiophene HDS activity versus CUS–Co/CUS–Mo and CUS CoMoS/CUS–Mo estimated from the area under the IR corresponding bands for CO (■) and NO (□) adsorption.

reveals that the number of Co exposed sites is higher than the number of CUS–Mo sites, suggesting a good level of Mo promotion by Co. The calculated CUS–Co/CUS–Mo ratio (see Table 4) indicates the best level of promotion for the Al_2O_3–MgO-supported catalyst. A plot of the CUS–Co/CUS–Mo ratio versus catalytic activity showed a linear relationship suggesting that promotion is responsible for the observed HDS (Fig. 4) catalytic activity. However, as mentioned before, the adsorption of NO is not completely reliable for providing information about the effectiveness of the promotion, because this technique does not distinguish the CUS–Co sites associated with the mixed CoMoS active phase from other Co sites. Therefore, the observed linear correlation between CUS–Co/CUS–Mo, obtained by NO adsorption, and catalytic activity might be fortuitous. The use of CO as a probe molecule provides information about Co involved in the promoted CUS–CoMoS sites [48]. Therefore, to corroborate the results obtained by NO, parallel CO chemisorption experiments were conducted on the sulfided catalysts.

4.3.2. CO adsorption

Fig. 5 shows the IR spectra around the C–O stretching region for the sulfided catalysts after CO adsorption at −173 °C. For $CoMoE/Al_2O_3$, bands at 2187, 2157, and ∼2080 cm^{-1}, with shoulders at around 2057 and 2100 cm^{-1}, are observed. The assignation of these bands and their shoulders was reported by Choi et al. [48]. The bands at 2187 and 2157 cm^{-1} are characteristic of CO adsorbed on the alumina support and are assigned to CO coordinated to Lewis acid sites (Al^{3+}) and CO in hydrogen bonding with the alumina hydroxyl groups, respectively.

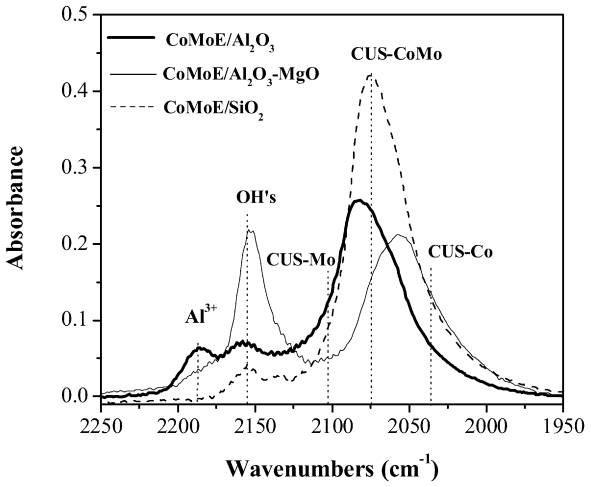

Fig. 5. FTIR spectra of CO adsorbed in the C–O stretching region for CoMoE sulfided catalysts on different supports at −173 °C and 1 Torr of CO at equilibrium.

The intense band and shoulders at lower frequency are characteristic of sulfided phases and are assigned to Co-promoted Mo sulfide sites (2080 cm^{-1}), Co sulfide sites (2057 cm^{-1}), and CO coordinated to CUS–Mo sites (2100 cm^{-1}). For $CoMoE/SiO_2$, CO adsorption gives rise to a band at 2155 cm^{-1} assigned to CO hydrogen bonded to the silica support OH groups and to an intense band at 2075 cm^{-1} (CUS–CoMoS), with shoulders at around 2110 (CUS–Mo) and 2060 cm^{-1} (CUS–Co).

After CO adsorption on $CoMoE/Al_2O_3$–MgO, the same number of bands is seen as for $CoMoE/Al_2O_3$ but, with important changes in their position and intensity. As Fig. 5 shows, the intensity of the band at 2155 cm^{-1} increased significantly (i.e., greater number of OH groups) and that of the band at 2187 cm^{-1} decreased (i.e., lower number of Al^{3+} sites) when magnesium was incorporated, indicating decreased support acidity.

The position of the CO bands, corresponding to sulfided sites, changed with the support. When the support changed from SiO_2 to Al_2O_3, the position of the CO bands shifted to higher wavenumbers. In contrast, for the Al_2O_3–MgO-supported catalyst, the CO bands shifted to lower wavenumbers. This behavior suggests electron enrichment around the Mo atoms involved in MoS_2 and CoMoS phases and could be a consequence of the increased basicity of the support surface [49]. Accordingly, for the alumina-supported catalyst, the observed shift toward higher wavenumbers indicates an electron deficiency around Mo, consistent with the higher acidity of alumina.

Because the adsorption of CO on sulfided CoMo catalysts distinguishes the promoted CoMoS sites from those associated only with Co or Mo, this probe molecule made it possible to obtain a more reliable level of promotion from the CUS–CoMoS/CUS–Mo ratio (Table 4). A plot of this ratio versus catalytic activity (also presented in Fig. 4) shows a linear relationship between CUS–CoMoS/CUS–Mo and HDS catalytic activity, in line with the NO adsorption experiments. These results indicate that the differences in catalytic activity are associated more closely with differences in the level of promotion

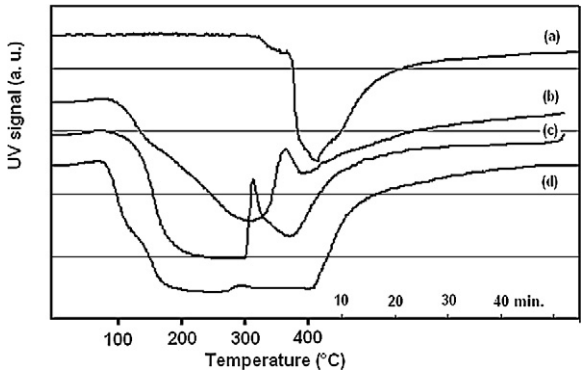

Fig. 6. TPS patterns of (a) Co–EDTA, unsupported (b) $CoMoE/Al_2O_3$, (c) $CoMoE/Al_2O_3$–MgO, (d) $CoMoE/SiO_2$.

than with changes in the dispersion degree of the MoS_2 phase. It appears, however, that the effectiveness of the chelating agent in improving the promotion of Mo by Co depends to a certain extent on the nature of the catalyst support. To investigate this issue, temperature-programmed sulfidation (TPS) experiments were conducted with the catalysts supported on the three different oxides.

4.4. Temperature-programmed sulfidation

Proper sulfidation of the active phase is of great importance to catalytic activity. To assess whether the type of support has some effect on the sulfidation behavior of the catalyst, TPS experiments were conducted with the three catalysts studied here. Fig. 6 shows the H_2S evolution curves for $CoMoE/Al_2O_3$, $CoMoE/Al_2O_3$–MgO, $CoMoE/SiO_2$, and the unsupported Co–EDTA complex.

Two H_2S consumption regions were detected for $CoMoE/Al_2O_3$–MgO and $CoMoE/Al_2O_3$. Although the temperatures for H_2S consumption and evolution are different, the shape of the curves are similar to those seen for conventional CoMo and NiMo catalysts supported on alumina without EDTA, for which the Mo reduction mechanism is well established [50]. Thus, the shape of the curves can be rationalized by considering that the first drop in the H_2S trace corresponds to the sequential sulfidation of Mo(6+) to MoO_2S, $MoOS_2$, and possibly MoS_3. The rise in the trace at 300–360 °C would then be related to the H_2S evolution caused by the reduction of some of these species into MoSO. The second H_2S consumption region at higher temperature is associated to the sulfidation of partially sulfided Mo(4+) species and the sulfidation of the Co promoter, which has been shifted to higher temperature because of its interaction with the EDTA ligand. As Fig. 6 shows, sulfidation of the unsupported Co–EDTA complex occurs at 380 °C and above. In contrast, sulfidation of Co(2+) supported on alumina has been reported to readily occur at low temperatures (∼180 °C) [10]. The difference in the temperatures at which H_2S consumption and evolution occur for each catalyst can be related to interactions of the Mo precursor with the support. For the Al_2O_3–MgO-supported catalyst, the H_2S evolution and consumption temperatures are shifted to lower values, indicating that AHM decomposes easier on Al_2O_3–MgO than on pure alumina. This result coincides

with a previous study on the decomposition of AHM on inert atmosphere on different supports (including Al_2O_3, SiO_2, and MgO) [34], which found that due to the depolymerization of AHM into tetrahedral MoO_4 moieties caused by the high IEP of MgO (∼12), AHM decomposed at lower temperatures on MgO than on Al_2O_3. In our case, an earlier sulfidation of AHM supported on the MgO-containing support would favor better promotion of MoS_2 by Co, which sulfides later due to its interaction with the chelating ligand [17,43].

The catalyst supported on SiO_2 shows a slightly different behavior. In this case, it appears that the two H_2S consumption regions overlap, and because of this, the H_2S evolution peak appears very small at 290 °C. It has been reported that because of the low IEP of SiO_2 (∼2.0), the decomposition of AHM/SiO_2 in inert atmospheres facilitates the formation of bulk-like MoO_3 species [33], which probably are highly dispersed. In our case, some MoO_3 is probably formed because in the TPS pattern of the SiO_2-supported catalyst, the peak representing the reduction of Mo(6+) to Mo(4+) appears at the same temperature (∼300 °C) as in a highly loaded MoO_3/Al_2O_3 catalyst [50], where most of the Mo is initially present in the form of MoO_3 particles. Because the Mo, Co, and EDTA contents were the same in all of the catalysts used here, the observed variations in sulfidation patterns are most likely related to differences in the interactions of the precursor phases with the support. Besides the interactions of the Co–EDTA complex, those of the Mo species with the support surface also could affect the sulfidation patterns. Increasing difficulty in sulfidation follows the order CoMoE/SiO_2 < CoMoE/Al_2O_3–MgO < CoMoE/Al_2O_3. Because the most active catalyst is CoMoE/Al_2O_3–MgO, it appears that, apart from the delay in sulfidation of the promoter, high HDS activity is favored by a medium support interaction, which promotes high dispersion while at the same time allowing good sulfidation. The HRTEM findings indicate that the Al_2O_3–MgO support induces smaller crystallites with a slightly lower level of stacking than those on alumina. In contrast, on SiO_2, large and highly stacked MoS_2 crystallites are observed.

5. Conclusion

CoMo catalysts supported on Al_2O_3 were prepared using various sequences of Co, Mo, and EDTA impregnation and tested in the HDS of thiophene. To assess the effect of the impregnation sequence and the effect of support on catalytic activity, the catalysts were characterized by different techniques. Based on the activity and characterization results, the following conclusions can be drawn.

The order of addition of Co, Mo, and EDTA during catalyst preparation has only a slight effect on HDS activity. The activity sequence (CoMoE) > Mo(Co + E) > Co(Mo + E) can be rationalized by the effectiveness of formation of the Co–EDTA complex and by the interactions of the active-phase precursors with the support. For catalysts prepared by simultaneous impregnation of Co, Mo, and EDTA, the HDS activity is significantly affected by variations in the nature of the support. Changing the support from Al_2O_3 to Al_2O_3–MgO makes the catalysts twice as active. The catalyst supported on SiO_2 leads to intermediate activity between the former supports. The ranking of the catalysts can be explained by differences in the level of Mo promotion by Co (NO and CO adsorption results) resulting from the delay in the Co sulfidation temperature with respect to Mo (TPS results). The extent of delay in the sulfidation of Co and Mo appears to be affected by the type of interactions of the Co–EDTA complex and the Mo precursor salt (AHM) with the supports used in this work. The type of support also affects the final dispersion of the MoS_2 crystallites (HRTEM results). Our findings indicate that the effectiveness of the chelating agent improving the promotion of Mo by Co depends to a certain extent on the nature of the catalyst support.

Acknowledgments

Financial support was provided by the IMP and DGAPA-UNAM (project IN-101406). The authors thank Ivan Puente for the HRTEM work and Roberto Sato for the Raman experiments.

References

[1] U.S. EPA, Control of Air Pollution from New Motor Vehicles: Heavy-Duty Engine and Vehicle Standards and Highway Diesel Fuel Sulfur Control Requirements: Final Rule, January 18, 2001; http://www.eia.doe.gov.
[2] M. Breysse, P. Afanasiev, C. Geantet, M. Vrinat, Catal. Today 86 (2003) 5.
[3] H. Topsøe, B.S. Clausen, F.E. Massoth, in: J.R. Anderson, M. Boudart (Eds.), Hydrotreating Catalysis Science and Technology, Springer-Verlag, New York, 1996, p. 11.
[4] J. Ramírez, G. Macías, L. Cedeño, A. Gutiérrez-Alejandre, R. Cuevas, P. Castillo, Catal. Today 98 (2004) 19.
[5] F. Luck, Bull. Soc. Chim. Belg. 100 (1991) 781.
[6] M. Breysse, G. Murali Dhar, C. Song, Catal. Today 86 (2003) 1.
[7] G. Murali Dhar, B.N. Srinivas, M.S. Rana, M. Kumar, S.K. Maity, Catal. Today 86 (2003) 45.
[8] H. Shimada, Catal. Today 86 (2003) 17.
[9] Y. Saih, K. Segawa, Catal. Today 86 (2003) 61.
[10] P. Arnoldy, J.L. de Booys, B. Scheffer, J.A. Moulijn, J. Catal. 96 (1985) 122.
[11] J.A.R. van Veen, E. Gerkema, A.M. van der Kraan, A. Knoester, J. Chem. Soc. Chem. Commun. (1987) 1684.
[12] L. Medici, R. Prins, J. Catal. 163 (1996) 28.
[13] R. Cattaneo, T. Shido, R. Prins, J. Catal. 185 (1999) 199.
[14] G. Kishan, L. Coulier, V.H.J. de Beer, J.A.R. van Veen, J.W. Niemantsverdriet, J. Catal. 196 (2000) 180.
[15] L. Coulier, G. Kishan, J.A.R. van Veen, J.W. Niemantsverdriet, J. Vac. Sci. Technol. A 19 (4) (2001) 1015.
[16] R. Cattaneo, F. Rota, R. Prins, J. Catal. 199 (2001) 318.
[17] L. Coulier, V.H.J. de Beer, J.A.R. van Veen, J.W. Niemantsverdriet, J. Catal. 197 (2001) 26.
[18] G. Kishan, J.A.R. van Veen, J.W. Niemantsverdriet, Top. Catal. 29 (2004) 103.
[19] G. Kishan, L. Coulier, V.H.J. de Beer, J.A.R. van Veen, J.W. Niemantsverdriet, J. Chem. Soc. Chem. Commun. (2000) 1103.
[20] S.M.A.M. Bouwens, J.A.R. van Veen, D.C. Koningsberger, V.H.J. de Beer, R. Prins, J. Phys. Chem. 95 (1991) 123.
[21] R. Cattaneo, Th. Weber, T. Shido, R. Prins, J. Catal. 191 (2000) 225.
[22] S.P.A. Louwers, R. Prins, J. Catal. 133 (1992) 94.
[23] G. Kishan, L. Coulier, J.A.R. van Veen, J.W. Niemantsverdriet, J. Catal. 200 (2001) 194.
[24] A.M. de Jong, V.H.J. de Beer, J.A.R. van Veen, E. Gerkema, J.W. Niemantsverdriet, J. Phys. Chem. (Lett.) 100 (45) (1996) 17722.

[25] L. Coulier, G. Kishan, J.A.R. van Veen, J.W. Niemantsverdriet, J. Phys. Chem. B 106 (2002) 5897.
[26] K. Hiroshima, T. Mochizuki, T. Honma, T. Shimizu, M. Yamada, Appl. Surf. Sci. 121/122 (1997) 433.
[27] P. Blanchard, C. Mauchaussee, E. Payen, J. Grimblot, O. Poulet, N. Biosdron, R. Loutaty, Stud. Surf. Sci. Catal. 91 (1995) 1037.
[28] P. Blanchard, E. Payen, J. Grimblot, O. Poulet, R. Loutaty, Stud. Surf. Sci. Catal. 111 (1997) 211.
[29] Y. Yoshimura, T. Sato, H. Shimada, N. Matsubayashi, M. Imamura, A. Nishijima, M. Higo, S. Yoshitomi, Catal. Today 29 (1996) 221.
[30] Y. Yoshimura, N. Matsubayashi, T. Sato, H. Shimada, A. Nishijima, Appl. Catal. A Gen. 79 (1991) 145.
[31] H. Shimada, T. Sato, Y. Yoshimura, J. Hiraishi, A. Nishijima, J. Catal. 110 (1988) 275.
[32] M.S. Rana, B.N. Srinivas, S.K. Maity, G. Murali Dhar, T.S.R. Prasada Rao, Stud. Surf. Sci. Catal. 127 (1999) 397.
[33] J. Rycskowski, Appl. Surf. Sci. 252 (2005) 813.
[34] C. Thomazeau, V. Martin, P. Afanasiev, Appl. Catal. A Gen. 199 (2000) 61.
[35] B. Caloch, M.S. Rana, J. Ancheyta, Catal. Today 98 (2004) 91.
[36] M.S. Rana, J. Ancheyta, P. Rayo, S.K. Maity, Catal. Today 98 (2004) 151.
[37] L.G. Silen, A.E. Martell, Stability Constants of Metal Complexes, vol. 2, Chem. Soc., London, 1964.
[38] J. Ramírez, S. Fuentes, G. Díaz, M. Vrinat, M. Breysse, M. Lacroix, Appl. Catal. 52 (1989) 211.
[39] H. Zhao, Z. Zhang, F. Shemsshaki, J. Zhang, Z. Ring, Energy Fuels 20 (2006) 1822.
[40] S.L. González-Cortés, T. Xiao, P.M.F.J. Costa, B. Fontal, M.L.H. Green, Appl. Catal. A Gen. 270 (2004) 209.
[41] X. Carrier, J.F. Lambert, M. Che, J. Am. Chem. Soc. 119 (1997) 10137.
[42] V. Sundaramurthy, A.K. Dalai, J. Adjaye, Catal. Lett. 102 (3–4) (2005) 299.
[43] R. Cattaneo, T. Shido, R. Prins, Stud. Surf. Sci. Catal. 127 (1999) 421.
[44] J. Ramírez, L. Ruíz Ramírez, L. Cedeño, V. Harle, M. Vrinat, M. Breysse, Appl. Catal. A Gen. 93 (1993) 163.
[45] L. Portela, P. Grange, B. Delmon, Catal. Rev. Sci. Eng. 37 (4) (1995) 699.
[46] N. Topsøe, H. Topsøe, J. Catal. 84 (1983) 386.
[47] T. Shimizu, K. Hiroshima, T. Honma, T. Mochizuki, M. Yamada, Catal. Today 45 (1998) 271.
[48] J.S. Choi, F. Maugè, C. Pichon, J. Olivier-Fourcada, J.C. Jumas, C. Petit-Clair, D. Uzio, Appl. Catal. A Gen. 267 (2004) 203.
[49] D. Mey, S. Brunet, C. Canaff, F. Maugé, C. Bouchy, F. Diehl, J. Catal. 227 (2004) 436.
[50] P. Arnoldy, J.A.M. van Den Heijkant, G.D. de Bok, J.A. Moulijn, J. Catal. 92 (1985) 35.